IEEE Access
Multidisciplinary | Rapid Review | Open Access Journal

Received January 4, 2020, accepted January 23, 2020, date of publication January 27, 2020, date of current version February 4, 2020.

Digital Object Identifier 10.1109/ACCESS.2020.2969678

Electromagnetic Force Distribution and Wall Thickness Reduction of Three-Coil Electromagnetic Tube Bulging With Axial Compression

LI QIU[1,2], (Member, IEEE), WANG ZHANG[1], A. ABU-SIADA[3], (Senior Member, IEEE), QI XIONG[1], (Member, IEEE), CHENGLIN WANG[1], YAO XIAO[1], BIN WANG[1], YANTAO LI[1,4], JINBO JIANG[1,2], AND QUANLIANG CAO[5]

[1]College of Electrical Engineering and New Energy, China Three Gorges University, Yichang 443002, China
[2]Hubei Provincial Key Laboratory for Operation and Control of Cascaded Hydropower Station, Yichang 443002, China
[3]Department of Electrical and Computer Engineering, Curtin University, Perth, WA 6102, Australia
[4]Hubei Provincial Yiling District Power Supply Company, Yichang 443100, China
[5]State Key Laboratory of Advanced Electromagnetic Engineering and Technology, Huazhong University of Science and Technology, Wuhan 430074, China

Corresponding authors: Jinbo Jiang (jinbojiang@163.com) and Quanliang Cao (quanliangcao@hust.edu.cn)

ABSTRACT In the conventional electromagnetic tube expansion, tube wall thickness tends to decrease significantly while the workpiece is expanded. This paper is aimed at introducing a new technique using three-coil electromagnetic tube bulging with axial compression as an innovative solution for this issue. To validate the feasibility of the proposed technique and investigate the electromagnetic force distribution along the workpiece, COMSOL software is used to construct a detailed finite element analysis model for the proposed electromagnetic coupling model. Results show that the ratio of the axial and the radial electromagnetic forces increases linearly with the increase of the height and the outer diameter of the top and bottom coils. Furthermore, the tube deformation profile and the wall thickness are compared with two different coil structures. Comparison analysis reveals that for the same axial to radial electromagnetic forces ratio, the effect of prohibiting the wall thickness reduction using different coil structures is quite similar. The new method is expected to have a good potential in enhancing the tube-forming performance.

INDEX TERMS Electromagnetic forming, tube bulging, axial electromagnetic force, tube wall thickness.

I. INTRODUCTION

Electromagnetic forming (EMF) is an industry technology that utilizes pulsed electromagnetic force to accelerate and deform metal workpieces [1]–[3]. The forming process is conducted in a time range of millisecond with a workpiece forming speed exceeding 300 m/s [4], [5]. Compared with conventional machining, EMF can improve the forming limit of materials [3], [6] and has become one of the recent hot research topics with a main goal of improving its performance [7].

The electromagnetic force during the EMF process is generated using a driving coil and the performance of the process can be assessed based on the distribution of this force over the workpiece. In 1958, the law of electromagnetic induction was applied to metal forming for the first time which paved the way to the EMF technology [8]. Since then, continuous improvements have been introduced to the EMF process. For instance, a uniform pressure coil technique which can generate homogeneous electromagnetic force on the workpiece was introduced in [9] to improve the poor deformation of sheet forming. In [10] a further improvement of sheet forming using electromagnetic force with local loading was presented. Based on the curved surface characteristic of the workpiece, a driving coil matching the structure of the workpiece was developed in [11].This coil can generate electromagnetic force that varies with the surface curvature of the workpiece and hence improving the efficiency of the electromagnetic forming. To realize the machining of large sheets, Cui *et al.* [12] proposed an electromagnetic

The associate editor coordinating the review of this manuscript and approving it for publication was Chan Hwang See.

incremental forming method. Various sets of power supplies were utilized to charge multiple driving coils to provide wide ranges of electromagnetic forces on the workpiece for long period [13]. This technique is known as space-time-controlled multi-stage pulsed magnetic field forming and manufacturing technology. To improve the radial flow in the electromagnetic sheet forming, Lai *et al.* [14] proposed an axial-radial bidirectional loading method. To overcome the issue of axial inhomogeneous deformation of tube bulging due to tube end effect, Qiu *et al.* [15] developed a concave driving coil to weaken the radial electromagnetic force in the middle of the tube and hence improving the tube forming quality. The electromagnetic bulging process of traditional solenoid coil is studied in [16], and the effect of tube length on the radial and axial magnetic pressures and highspeed deformation are discussed. Reference [17] explores the effect of coil length and relative position on the deformation profile of tube electromagnetic bulging, which does not involve the thinning of wall thickness. In [18], the electromagnetic bulging is carried out using multi-directional magnetic pressure, which significantly increases the axial feed of the pipe and reduces the thickness of the easy-to-break part.

From the above discussion, changing the loading mode of the electromagnetic force can improve the forming performance and efficiency to a certain extent. However, for electromagnetic tube expansion, the tube wall thickness reduction is still a point of concern that needs further improvement to enhance the tube forming quality.

Aiming at this point, an electromagnetic tube expansion with axial compression was proposed in [19], [20]. The main contribution of this paper is the presentation of detailed investigation for the influence of different system parameters on the electromagnetic force distribution and wall thickness reduction of the electromagnetic tube forming process. In this context, an electromagnetic-structural coupling model emulating the practical process is developed and analyzed. The effect of the axial and radial electromagnetic forces distribution on the tube is investigated through the relative thickness reduction coefficient as will be explained below.

II. PRINCIPLE OF ELECTROMAGNETIC TUBE BULGING WITH AXIAL COMPRESSION

The basic principle of the electromagnetic tube expansion is shown in the schematic of Fig. 1. In the tube forming process, the electrical energy stored in the capacitor shown in Fig. 1 is released instantly to the driving coil to produce a pulse current. This results in an induced eddy current in the metal tube based on the principle of electromagnetic induction. The pulsed electromagnetic force due to the interaction of the magnetic flux and the induced eddy current drives the tube to accelerate and deform.

Due to the axial symmetry of the coil and the tube, the electromagnetic tube expansion process can be simplified to a two-dimensional axial symmetrical model. The eddy current density in the workpiece mainly flows in the circumferential

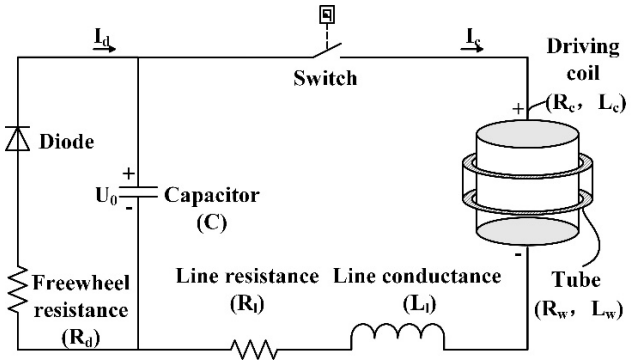

FIGURE 1. Schematic diagram of the electromagnetic tube bulging system.

direction based on the below equations.

$$\nabla \times \boldsymbol{E}_{\varphi} = -\frac{\partial \boldsymbol{B}_z}{\partial \boldsymbol{t}} + \nabla \times (\boldsymbol{v}_z \times \boldsymbol{B}_r) \tag{1}$$

$$\boldsymbol{J}_{\varphi} = \gamma \boldsymbol{E}_{\varphi} \tag{2}$$

where $\boldsymbol{E}$ is the electric field intensity, $\boldsymbol{B}$ is the magnetic flux density, $\boldsymbol{v}$ is the speed of the workpiece, $\boldsymbol{J}$ is the induced eddy current intensity, $\boldsymbol{\gamma}$ is the electrical conductivity of the workpiece. Subscripts $\boldsymbol{r}$, φ and z are respectively the radial, hoop, and axial components of the variable.

The radial and axial electromagnetic forces acting on the tube during the forming process can be calculated from:

$$\boldsymbol{F}_r = \boldsymbol{J}_{\varphi} \times \boldsymbol{B}_z \tag{3}$$

$$\boldsymbol{F}_z = \boldsymbol{J}_{\varphi} \times \boldsymbol{B}_r \tag{4}$$

From (3) and (4), the radial electromagnetic force $\boldsymbol{F}_r$ is calculated based on the hoop eddy current and the axial magnetic flux density whereas the axial electromagnetic force $\boldsymbol{F}_z$ is determined using the hoop eddy current and the radial magnetic flux density.

Based on Newton's law, the force and displacement of the tube satisfy the following equation:

$$\nabla \cdot \sigma + \boldsymbol{F} = \rho \frac{\partial^2 \boldsymbol{u}}{\partial \boldsymbol{t}^2} \tag{5}$$

where σ is the stress tensor of the tube, $\boldsymbol{F}$ is the bulk density vector of the electromagnetic force, ρ is the tube density and $\boldsymbol{u}$ is the displacement vector.

Cowper-Symonds model is used to simulate the tube based on the following equations:

$$\sigma_{ys} = \begin{cases} E\varepsilon & \sigma_{ys} < \sigma_{yso} \\ \sigma_{ys0} + A\varepsilon_{pe}^{B} & \sigma_{ys} \geq \sigma_{yso} \end{cases} \tag{6}$$

$$\sigma = [1 + (\frac{\varepsilon_{pe}}{C_m})^m]\sigma_{ys} \tag{7}$$

where E is the young's modulus, σ is the flow stress when the tube material deforms at high speed, m is the strain rate hardening parameter, C_m is the viscosity parameter. A and B are constants; 90.5 and 0.35, respectively and σ_{yso} is the

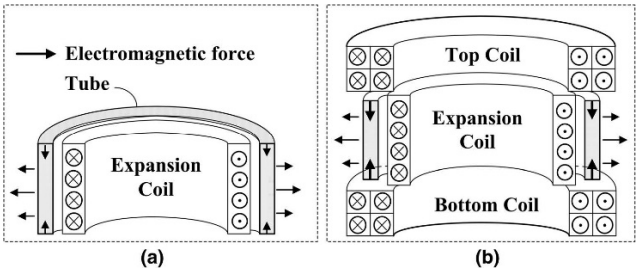

FIGURE 2. Electromagnetic forming system. (a) Conventional 1-coil topology, (b) proposed 3-coil topology.

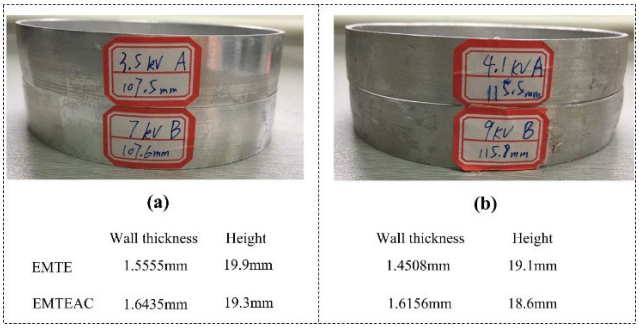

	Wall thickness	Height	Wall thickness	Height
EMTE	1.5555mm	19.9mm	1.4508mm	19.1mm
EMTEAC	1.6435mm	19.3mm	1.6156mm	18.6mm

FIGURE 3. Experimental comparison of wall thickness of the conventional topology (EMTE) and the proposed topology (EMTEAC) [20].

initial yield stress of the workpiece, ε_{pe} is the plastic strain. $C_m = 6500$, $m = 0.25$ are usually used for aluminum.

In the current conventional electromagnetic tube expansion (Fig. 2(a)), only a small amount of radial magnetic flux intensity is produced at the end of the tube due to the end effect [20]. Consequently, the axial force acting on the tube is very small and the radial electromagnetic force dominates the forming process of the workpiece. This results in a serious thickness reduction in the tube wall that reduces the mechanical strength of the tube significantly.

To solve this issue, two additional coils are introduced at the top and bottom of the tube as shown in Fig. 2(b) to form a new topology known as three-coil electromagnetic tube bulging with axial compression. This topology can significantly strengthen the radial magnetic flux intensity over the entire tube and hence improving the axial electromagnetic force. The axial force causes the tube to flow in axial direction and helps reducing the phenomenon of tube wall thickness reduction in the conventional single coil topology. Experimental results published in [20] are shown in Fig. 13. As shown in Figure 3(a), with a bulging amount of 107.5-107.6 mm, the tube wall thickness is reduced from 2 mm to 1.5555 mm under conventional electromagnetic tube expansion (EMTE) while it decreases to 1.6435 mm when the proposed axial compression (EMTEAC) is used. For another tube shown in Figure 3(b) and for a bulging amount of 115.5-115.8 mm, the wall thickness reduces from 2 mm to 1.4508 mm under EMTE while decreases to 1.6156 mm under EMTEAC. These results indicate the proposed method reduces the decrease in wall thickness from 27 to 19%.

III. ELECTROMAGNETIC-STRUCTURAL COUPLING MODEL FOR THE ELECTROMAGNETIC TUBE BULGING PROCESS

In order to analyze the electromagnetic force distribution and the phenomenon of tube wall thickness reduction during the electromagnetic bulging process, a finite element model of the tube expansion process is developed using COMSOL software.

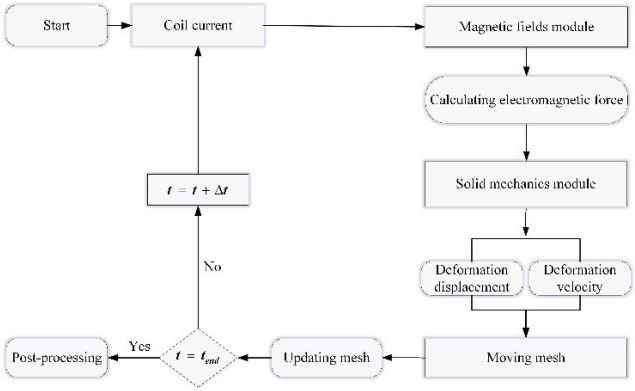

FIGURE 4. Flow chart of the simulation model.

Fig. 4 shows the flow chart of the simulation process. In the simulation model, the external current density of the driving coil is set and the axial and radial electromagnetic forces acting on the tube are calculated using the magnetic field model. The elastic-plastic deformation process of the tube is simulated using a solid mechanics model. Moving mesh module is employed to update the finite element mesh deformed due to the bulging process. The outer boundary of the near field air domain and the coil domain boundary are assumed to be fixed and the near field air and the tube domains are considered of free deformations. Because the maximum radial bulging amount in this paper is about 9 mm, the finite element mesh changes with the tube outward expansion. In order maintain the mesh quality and distortion after deformation, a moving mesh module is added to the simulation model to constantly update the bulging mesh.

The last step in the modelling is to compare the execution time with the pre-set time in order to repeat the calculation or end the process and analyze the results. While this model has been experimentally validated in the authors' previous paper [20], detailed effects of various parameters on the model's performance are investigated in this paper.

Geometrical dimensions of the developed single -coil and three-coil electromagnetic forming systems are shown in Fig. 5. The inner diameter of the tube is 30 mm with a height of 20 mm and thickness of 5 mm. The used coils are of copper wire with a rectangular cross section of $2 \times 4\ mm^2$. Tube material parameters are: density ($2750\ kg/m^3$), electrical conductivity (3.6×10^7 S/m), initial yield tensile strength (50 MPa), Poisson's ratio (0.3) and Young's modulus (71.5 GPa).

As this paper is aimed at investigating the effect of various coil heights and diameters on the electromagnetic force and

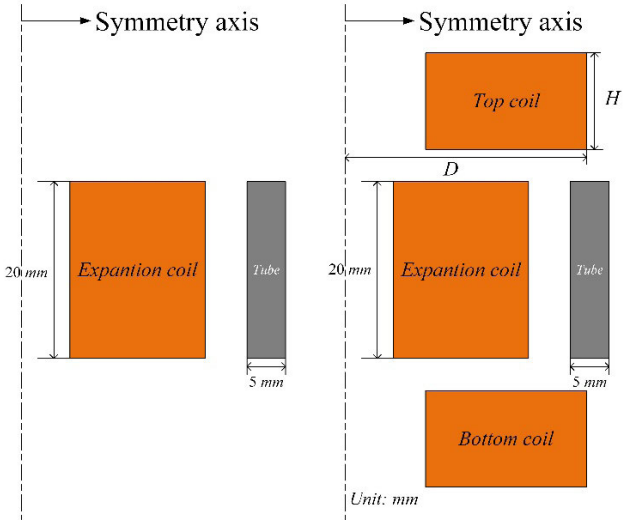

FIGURE 5. Geometrical dimensions of tube electromagnetic bulging. (a) Conventional 1-coil, (b) proposed 3-coil topology.

tube wall thickness, finite element analysis of the process which emulates physical systems is developed.

IV. DISTRIBUTION CHARACTERISTIC OF THE ELECTROMAGNETIC FORCE

As discussed above, the electromagnetic distribution of the single coil topology is modified by introducing top and bottom coils. Hence, this section is aimed at investigating the influence of coils physical geometry on the electromagnetic force distribution. The initial parameters of the three-coil system are listed in Table 1.

TABLE 1. Initial parameters of the three-coil system; unit (mm).

Structure parameter	
Height of top-bottom coil	8
Outer diameter of top-bottom coil	32
Inner diameter of top-bottom coil	20
Height of expansion coil	20
Outer diameter of expansion coil	26
Inner diameter of expansion coil	10

A. EFFECT OF COIL HEIGHT

In order to explore the influence of the height $\boldsymbol{H}$ of the top-bottom coil on the electromagnetic force distribution, the coil height is varied while maintaining all other physical parameters. Fig. 6(a) shows the distribution of the radial electromagnetic force $\boldsymbol{F}_r$ as a function of time at different coil heights while Fig. 6(b) shows the peak value of the radial electromagnetic force $\boldsymbol{F}_{rp}$ at different coil heights. These results reveal that the radial electromagnetic force increases gradually with the increase in the coil height and the peak force is linearly correlated with the coil height when it is less than 10 mm. The incremental rate of the peak radial

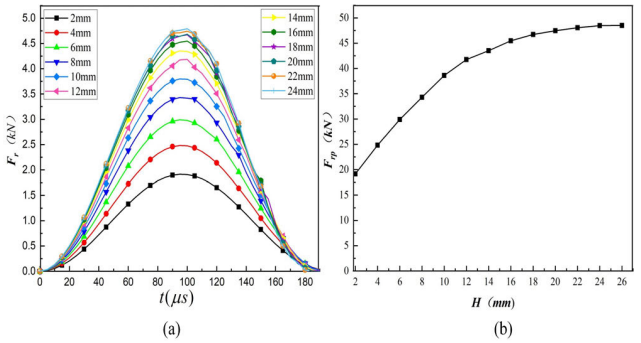

FIGURE 6. Effect of various coil height (legend) on the electromagnetic force. (a) Radial electromagnetic force, (b) peak value of the radial electromagnetic force versus coil height.

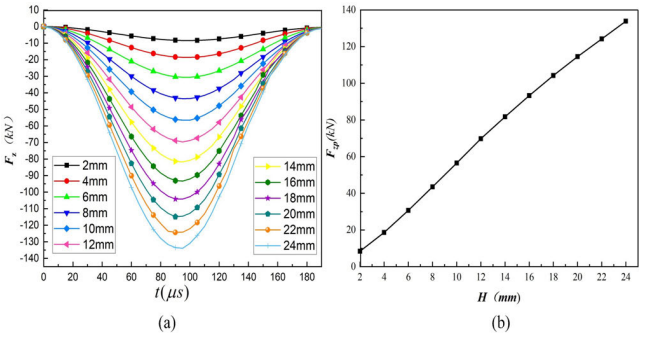

FIGURE 7. Effect of various coil heights (legend) on the electromagnetic force. (a) Axial electromagnetic force, (b) peak value of the axial electromagnetic force versus coil height.

electromagnetic force slows down and eventually tends to saturate for coil heights larger than 10 mm. Results in Fig. 6(a) also show that for all coil heights, the peak radial force takes place at the middle of the processing time (100 μs).

The distribution characteristics of the axial electromagnetic force $\boldsymbol{F}_z$ as a function of the execution time at different coil heights is shown in Fig. 7(a) with a peak values $\boldsymbol{F}_{zp}$ as a function of the coil height as shown in Fig. 7(b). Results show that the amplitude of the axial electromagnetic force also increases gradually with the increase of the coil height till it reaches a crest value at almost the middle of the process execution time. It can be also observed that the peak axial force is almost of a linear correlation with the height of the top-bottom coil.

In order to further explore the influence of the height of the top-bottom coil on the electromagnetic distribution characteristics, the ratio between the peak values of the axial and radial forces at different coil heights is investigated as shown in Fig. 8. It can be seen that the ratio $\boldsymbol{F}_z/\boldsymbol{F}_r$ increases linearly with the coil height, in particular after 10 mm because saturation takes place in the radial electromagnetic force after 10 mm coil height.

B. EFFECT OF COIL OUTER DIAMETER

This effect is investigated by changing the coil outer diameter in a wide range while maintaining all other coil physical

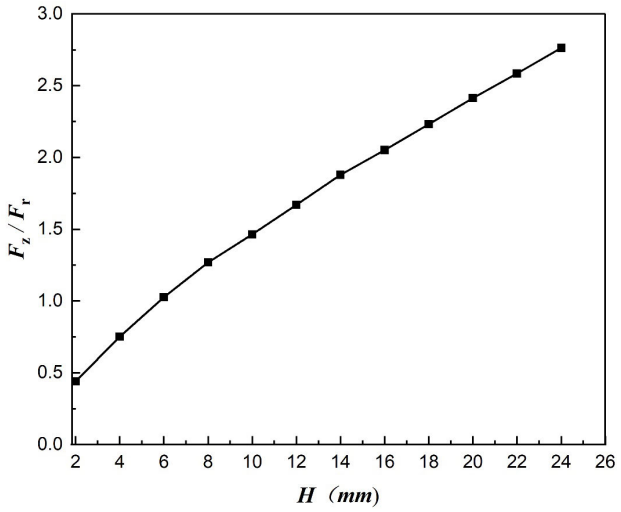

FIGURE 8. The ratio F_z/F_r at different coil heights H.

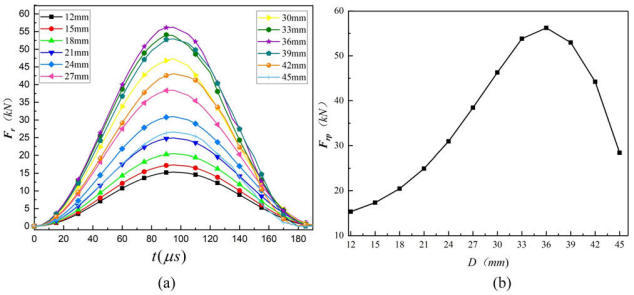

FIGURE 9. Effect of various coil outer diameter (legend) on the electromagnetic force (a) Radial electromagnetic force, (b) peak value of the radial electromagnetic force versus coil diameter.

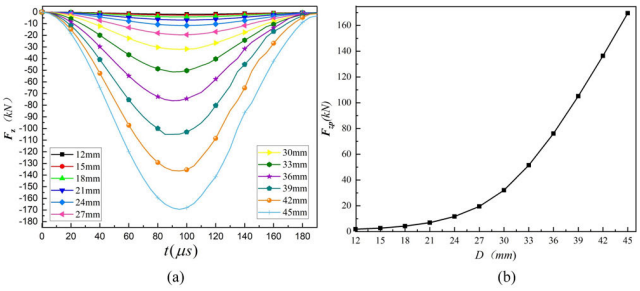

FIGURE 10. Effect of various coil outer diameter (legend) on the electromagnetic force (a) Axial electromagnetic force, (b) peak value of the axial electromagnetic force versus coil diameter.

parameters. Fig. 9(a) shows the radial electromagnetic force $\boldsymbol{F}_r$ as a function of time at different coil outer diameter $\boldsymbol{D}$. Fig. 9(b) shows the peak radial force as a function of $\boldsymbol{D}$. These results reveal that $\boldsymbol{F}_r$ increases when the coil outer diameter increases until $\boldsymbol{D}$ reaches 35 mm, for this model, after which $\boldsymbol{F}_r$ decreases with the increase of the outer diameter. This characteristic is attributed to the fact that there is a reverse compressive radial electromagnetic force acting on the inside of the tube when the coil outer diameter becomes greater than a critical value (35 mm in the investigated model).

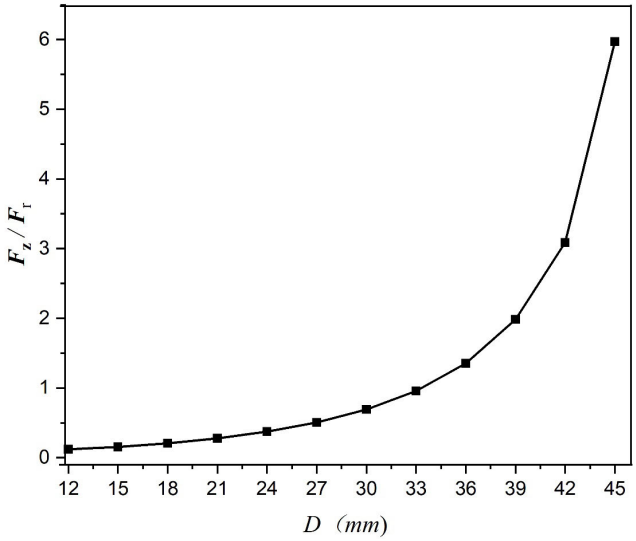

FIGURE 11. The ratio F_z/F_r at different coil outer diameters D.

Fig. 10(a) shows the time profile of the axial electromagnetic force $\boldsymbol{F}_z$ at different coil outer diameters and Fig. 10(b) shows the peak value of the axial electromagnetic force $\boldsymbol{F}_{zp}$ at coil different outer diameters. The two plots reveal that the larger the outer diameter of the top-bottom coil is, the stronger the axial electromagnetic force becomes. Also, the peak value of the axial electromagnetic force increases slowly when the outer diameter of the coil is less than 25 mm after which it increases quadratically with the increase in the coil outer diameter.

Fig. 11 shows the ratio $\boldsymbol{F}_z/\boldsymbol{F}_r$ increases in a similar fashion to the peak value of the axial force which is attributed to the reduced radial electromagnetic force for coil outer diameters larger than 35 mm.

V. WALL THICKNESS REDUCTION

A relative tube wall thickness reduction coefficient $\boldsymbol{K}$ during the electromagnetic bulging process is calculated as:

$$\boldsymbol{K} = \frac{\boldsymbol{R}_{EMTEAC}}{\boldsymbol{R}_{EMTE}} \tag{8}$$

where $\boldsymbol{R}_{EMTEAC}$ and $\boldsymbol{R}_{EMTE}$ are the wall thickness reduction at the central-node of the tube inner wall using the proposed three-coil topology and the conventional single-coil electromagnetic tube bulging topology; respectively.

Small values of $\boldsymbol{K}$ reveal better performance of the proposed method than the conventional method. This coefficient is usually less than 1 due to the impact of axial compression.

A. INFLUENCE OF COIL HEIGHT ON WALL THICKNESS REDUCTION

The tube wall thickness behavior is investigated by changing the height of the top-bottom coil while maintaining all other coil physical parameters. The profiles of the central-node deformations at the tube inner wall $\boldsymbol{D_i}$ and the tube outer wall $\boldsymbol{D_o}$ are obtained as shown in Figs. 12(a) and 12(b);

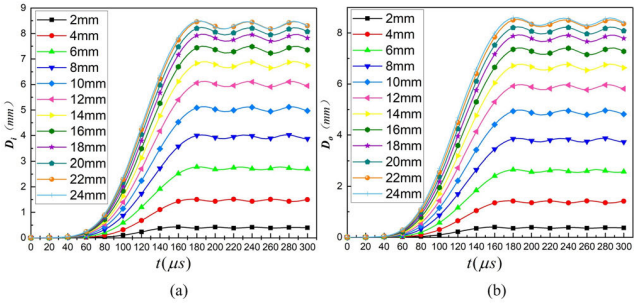

FIGURE 12. Effect of coil height (legend) on deformation. (a) D_i deformation, (b) D_o deformation.

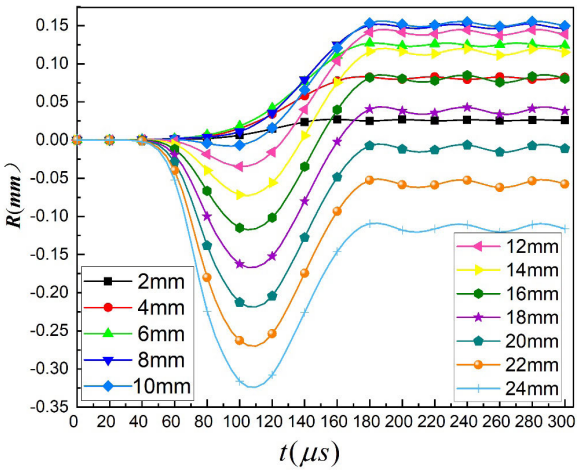

FIGURE 13. Tube wall thickness reduction at different coil heights (legend).

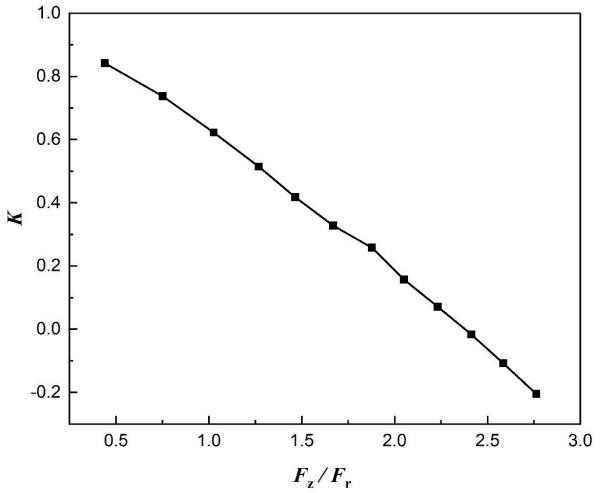

FIGURE 14. The value K versus F_z/F_r ratio calculated at different coil heights.

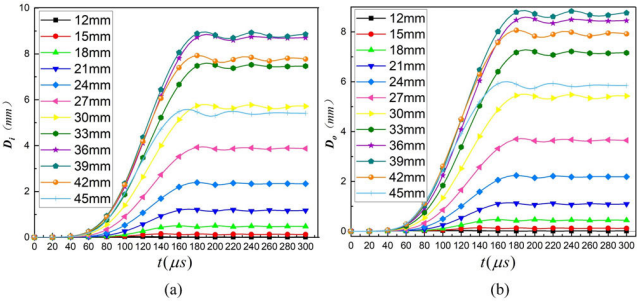

FIGURE 15. Effect of coil outer diameter on deformation. (a) Inner wall deformation, (b) outer wall deformation.

respectively. Results show that both D_i and D_o increase with the increase in coil height. The wall thickness reduction R at the central-node of the tube is obtained by subtracting D_o from D_i as shown in Fig. 12.

Obviously, the effect of the coil height on wall thickness reduction cannot be directly acquired from Fig. 13 as the bulging amount of the tube inner wall is disparate. Therefore, the tube wall thickness reduction when a conventional single coil and the proposed three-coil topologies is obtained through adjusting the current of the driving coil. Various values of K are calculated at different coil heights as shown in Fig. 14 that correlates the ratio F_z/F_r with the tube wall thickness reduction coefficient K. It can be seen that the coefficient K decreases with the increase of the ratio F_z/F_r,which demonstrates the effect of prohibiting wall thickness reduction by controlling this ratio through controlling the physical dimensions of the used coils.

B. INFLUENCE OF COIL OUTER DIAMETER ON WALL THICKNESS REDUCTION

The tube wall thickness during the electromagnetic forming process is investigated by changing the coil outer diameter with keeping other parameters unchanged. The profiles of the central-node deformation at the tube inner wall D_i and outer wall D_o are obtained for this case study as shown in Figs. 15(a) and 15(b); respectively. The tube wall thickness reduction time profile R at different coil outer diameters is shown in Fig. 16. The variation trend of the coefficient K with the ratio F_z/F_r shown in Fig. 17 is to the trend shown in Fig. 14. Both plots are compared as shown in Fig. 18 which shows that the two trends are almost identical. This indicates that either coil height or diameter can be controlled to control the wall thickness of the workpiece as long as the ratio F_z/F_r is maintained.

VI. WALL THICKNESS REDUCTION UNDER SAME F_Z/F_r RATIO

The above analysis shows that the wall thickness of the tube can be reduced by the same amount through changing either the coil outer diameter or height while maintaining the F_z/F_r ratio. Two physical dimension sets of the proposed method as shown in Table 2 are selected to investigate the effect of different coil structures on tube formability under the same F_z/F_r ratio. To maintain consistency, the amplitude of the coil current density of structures 1 and 2 are set as $0.867 \times 10^9 A/m^2$ and $1.2 \times 10^9 A/m^2$, respectively.

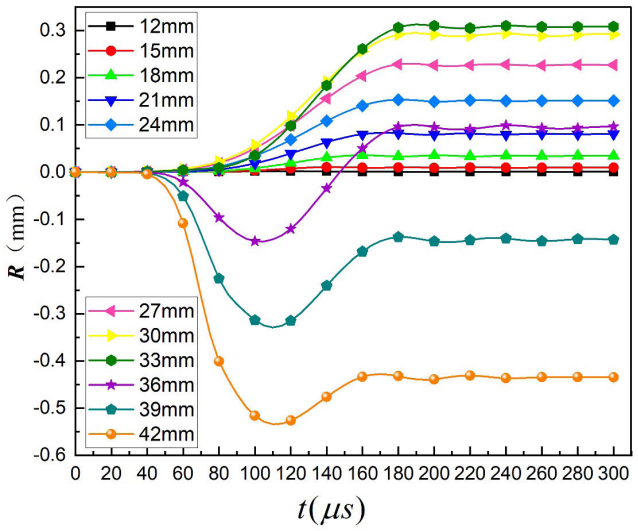

FIGURE 16. Wall thickness reduction (*R*) of the tube at different coil outer diameters (legend).

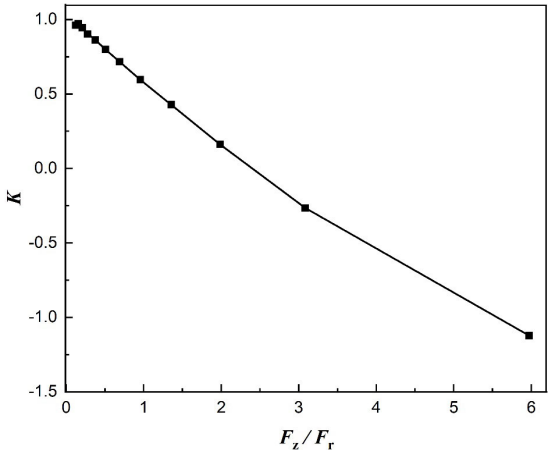

FIGURE 17. The value *K* versus F_z/F_r *ratio calculated at different coil outer diameters.*

A. ELECTROMAGNETIC FORCE DENSITY PROFILE

The radial electromagnetic force generated on the tube is correlated with the axial magnetic flux density whereas the axial electromagnetic force is determined by the radial magnetic flux density. The electromagnetic force density distribution of structures 1 and 2 at different times are respectively shown in Figs. 19 and 20, respectively. These results show that the distribution of the electromagnetic force density with two different coil structures are consistent, which means the direction and amplitude of the electromagnetic force stay in reasonable agreement for both structures.

B. CHARACTERISTICS OF WORKPIECE FORMING VELOCITY

Because electromagnetic force drives the workpiece during the forming process, deformation velocity at different times is investigated to compare the formability performance of

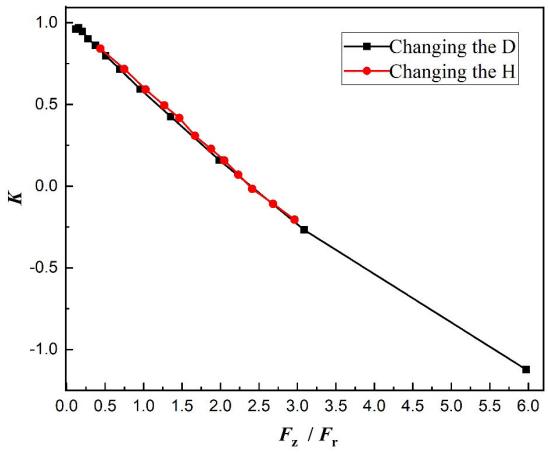

FIGURE 18. Comparison of the trend of *K* in figures 14 and 17.

TABLE 2. Two sets of coil structures with the same F_z/F_r (unit mm).

Structure parameter \ Structure	1	2
Height of top-bottom coil	24	8
Outer diameter of top-bottom coil	32	39
Inner diameter of top-bottom coil	20	20
Height of expansion coil	20	20
Outer diameter of expansion coil	26	26
Inner diameter of expansion coil	10	10

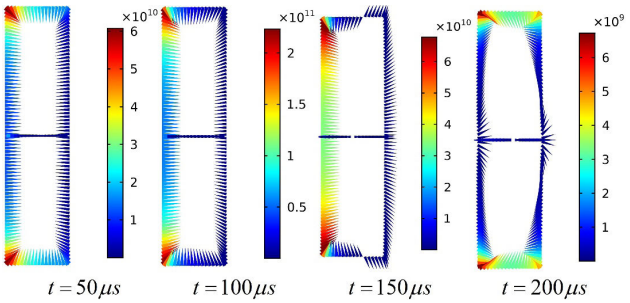

FIGURE 19. Electromagnetic force density of structure 1 at different times (unit N/m^3).

the two structures. Compared with the traditional single coil electromagnetic forming, the workpiece under the proposed electromagnetic tube bulging with axial compression not only exhibits a radial expansion, but also an axial flow, thereby reducing the wall thickness thinning. Fig. 21 shows the electromagnetic-structural coupling model employed in this paper. In order to analyze the flow characteristics of the workpiece under the loading model of structures 1 and 2, six points; A, B, C, D, E and F as shown in Fig. 21 are selected to investigate the deformation velocity of the tube.

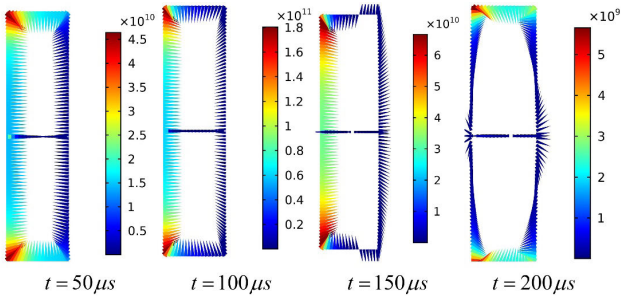

FIGURE 20. Electromagnetic force density of structure 2 at different times (unit N/m^3).

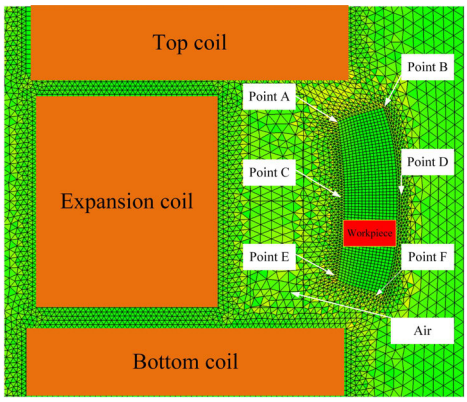

FIGURE 21. Developed electromagnetic-structural coupling model.

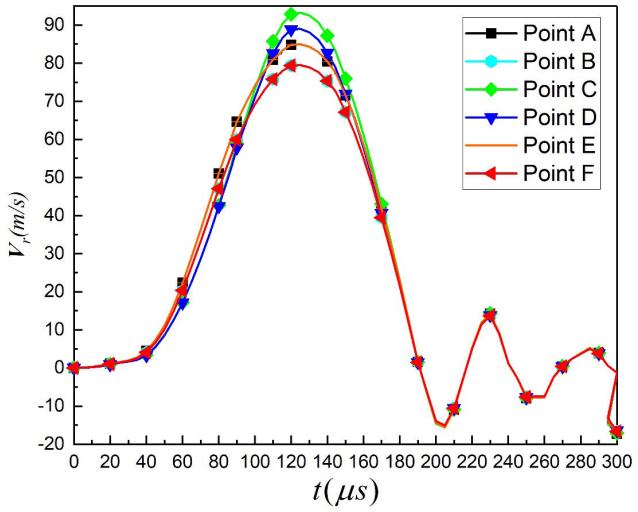

FIGURE 22. Radial forming velocity for structure 1 at different model positions.

Figures 22 and 23 show the radial forming velocity V_r at different positions for structures 1 and 2, respectively. It can be seen that V_r increases continuously and reaches a maximum value at 125 μs then decreases to 0 at 190 μs for all investigated points in both structures. It is to be noted that deformation rate less than zero indicates workpiece is exhibiting a springback effect. Compared with the traditional

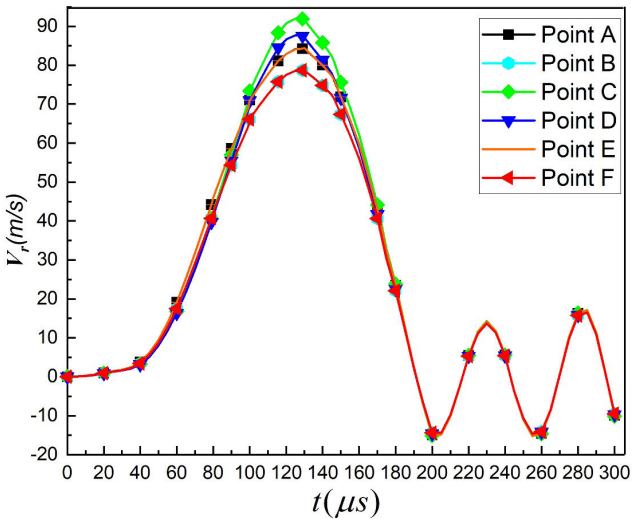

FIGURE 23. Radial forming velocity for structure 2 at different model positions.

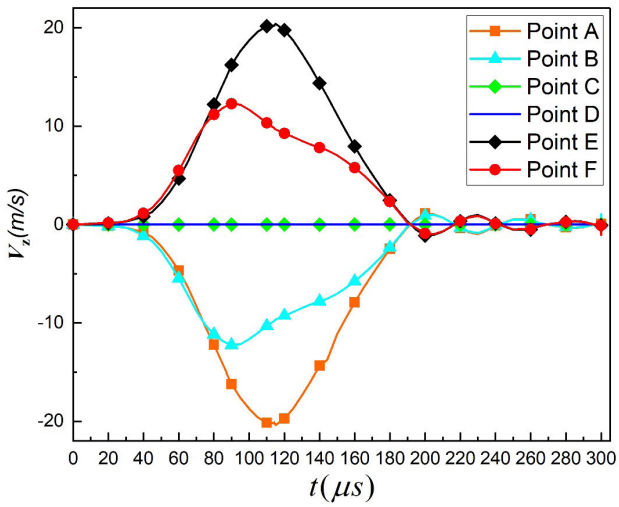

FIGURE 24. Axial forming velocity of structure 1 at different model positions.

quasi-static, electromagnetic forming technology can restrain the springback of materials more effectively [21]. This paper mainly explores the tube free electromagnetic bulging process, in which the radial bulging oscillates then settles at a steady state level which is used in the calculation. Electromagnetic forming technology can deform at high strain rate, produce better formability, reduce springback effect and improve the forming limit of the material [22]. The radial deformation rate curves for points A, E and for points B, F are overlapped because of their symmetrical locations. The maximum V_r of points A, B, C, and D in structure 1 are 84.95 m/s, 79.5 m/s, 93.24 m/s, and 88.98 m/s; respectively. On the other hand, the maximum V_r of points A, B, C, and D in structure 2 are 84.17 m/s, 78.53 m/s, 92 m/s, 87.68 m/s; respectively. The difference of the V_r peak values for both structures at different positions is less than 2%.

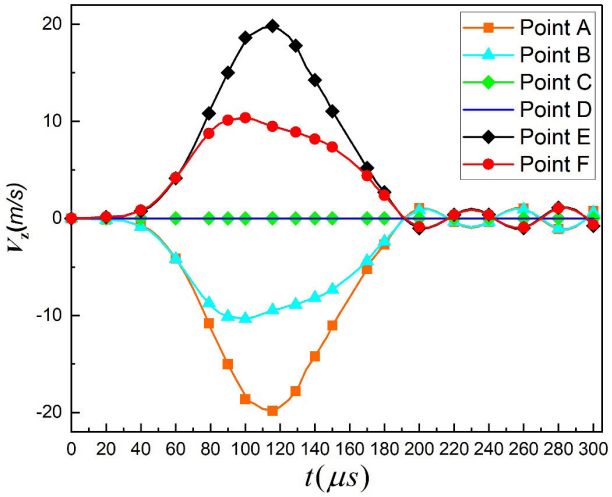

FIGURE 25. Axial forming velocity of structure 2 at different model positions.

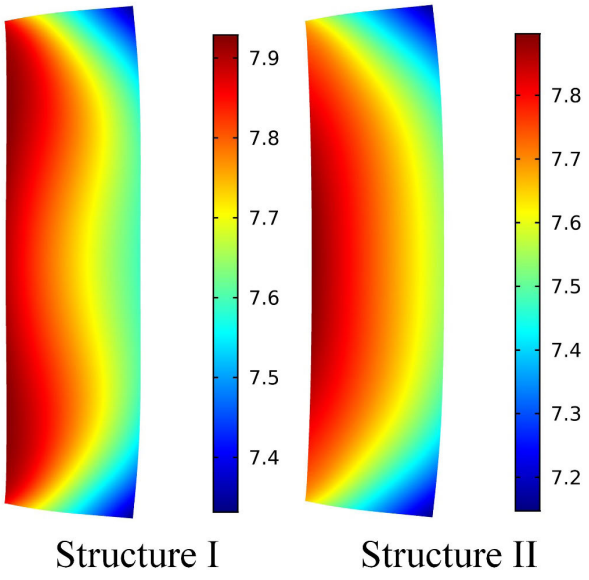

FIGURE 26. The 2-D deformation profile of the two investigated structures.

Figures 24 and 25 show the axial forming velocity $\boldsymbol{V}_z$ for structure 1 and 2 at different positions. The axial forming rate at points C and D are always zero since they are located along the x-axis of the model. The amplitudes of $\boldsymbol{V}_z$ at points A, E and points B, F are the same, but opposite in direction due to their geometrical symmetry. The maximum $\boldsymbol{V}_z$ of point A and B in structure 1 are 20.2 m/s and 12.3 m/s, respectively while they are 19.86 m/s and 10.36 m/s, respectively for structure 2. The difference between the peak values of $\boldsymbol{V}_z$ for the two structures at different positions is also less than 2%.

Based on the obtained results, it can be concluded that the axial and radial flow of the workpiece are the same regardless the model structure when the ratio $\boldsymbol{F}_z/\boldsymbol{F}_r$ is kept constant.

The two-dimensional deformation profile and the tube wall thickness reduction for the two investigated structures are obtained as shown in Figures 26 and 27, respectively.

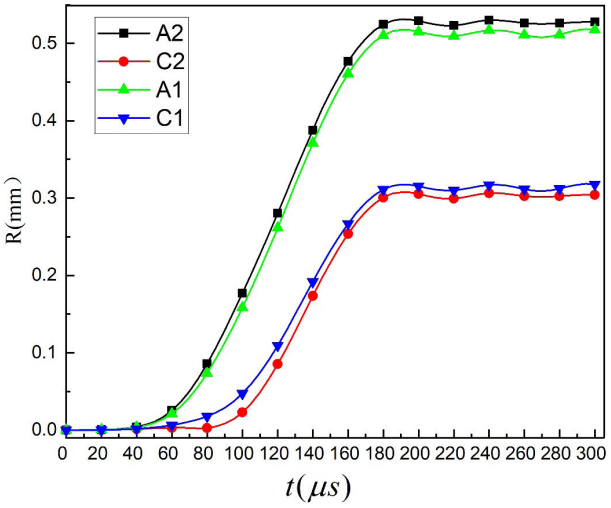

FIGURE 27. Wall thickness reduction using the two investigated structures at positions A and C on the model.

Obviously, the deformed profiles using the two structures are of great similarity while wall thickness reduction shows a little difference. In summary, the tube-forming performance entirely coincides when the tube exhibits electromagnetic force generated by different coil structures while maintaining the $\boldsymbol{F}_z/\boldsymbol{F}_r$ ratio, and so as the wall thickness reduction.

VII. CONCLUSION

In order to solve the thinning problem of the wall thickness in the conventional tube bulging, this paper presents a detailed investigation of a new three-coil electromagnetic tube bulging with axial compression method. In this context, COMSOL software is used to establish a detailed electromagnetic-structural coupling model for the proposed method. The following conclusions can be drawn from the obtained results:

- Different axial electromagnetic force loadings can be achieved by modifying the geometry of the two additional top and bottom coils.
- The wall thickness reduction of the tube can be suppressed when the axial and the radial electromagnetic forces are loaded bidirectionally.
- The difference in tube wall thickness obtained using different coil structures is relatively small when the ratio $\boldsymbol{F}_z/\boldsymbol{F}_r$ is kept constant.
- Coil geometrical dimensions including height and outer diameter can be optimized to improve the performance of the proposed three-coil electromagnetic tube bulging process.

The new technique is paving the way for further improvements in this field of research that has become of a great concern to industry and researchers alike.

REFERENCES

[1] Q. Cao, Z. Li, Z. Lai, Z. Li, X. Han, and L. Li, "Analysis of the effect of an electrically conductive die on electromagnetic sheet metal forming process using the finite element-circuit coupled method," *Int. J. Adv. Manuf. Technol.*, vol. 101, nos. 1–4, pp. 549–563, Mar. 2019.

[2] L. Qiu, Y. Li, Y. Yu, A. Abu-Siada, Q. Xiong, X. Li, L. Li, P. Su, and Q. Cao, "Electromagnetic force distribution and deformation homogeneity of electromagnetic tube expansion with a new concave coil structure," *IEEE Access*, vol. 7, pp. 117107–117114, 2019.
[3] Q. Xiong, H. Tang, M. Wang, H. Huang, L. Qiu, K. Yu, and Q. Chen, "Design and implementation of tube bulging by an attractive electromagnetic force," *J. Mater. Process. Technol.*, vol. 273, Nov. 2019, Art. no. 116240.
[4] Q. Cao, L. Du, Z. Li, Z. Lai, Z. Li, M. Chen, X. Li, S. Xu, Q. Chen, X. Han, and L. Li, "Investigation of the Lorentz-force-driven sheet metal stamping process for cylindrical cup forming," *J. Mater. Process. Technol.*, vol. 271, pp. 532–541, Sep. 2019.
[5] L. Qiu and K. Deng, "Analysis of coil temperature rise in electromagnetic forming with coupled cooling method," *Int. J. Appl. Electromagn. Mech.*, to be published.
[6] L. Qiu, Y. Xiao, C. Deng, Z. Li, Y. Xu, Z. Li, and P. Chang, "Electromagnetic-structural analysis and improved loose coupling method in electromagnetic forming process," *Int. J. Adv. Manuf. Technol.*, vol. 89, nos. 1–4, pp. 701–710, Mar. 2017.
[7] S. Ouyang, X. Li, C. Li, L. Du, T. Peng, X. Han, L. Li, Z. Lai, and Q. Cao, "Investigation of the electromagnetic attractive forming utilizing a dual-coil system for tube bulging," *J. Manuf. Processes*, vol. 49, pp. 102–115, Jan. 2020.
[8] Q. Cao, X. Han, Z. Lai, Q. Xiong, X. Zhang, Q. Chen, H. Xiao, and L. Li, "Analysis and reduction of coil temperature rise in electromagnetic forming," *J. Mater. Process. Technol.*, vol. 225, pp. 185–194, Nov. 2015.
[9] M. Kamal and G. S. Daehn, "A uniform pressure electromagnetic actuator for forming flat sheets," *J. Manuf. Sci. Eng.*, vol. 129, no. 2, pp. 369–379, Apr. 2007.
[10] L. Qiu, Y. Yu, Y. Yang, X. Nie, Y. Xiao, Y. Ning, F. Wang, and C. Cao, "Analysis of electromagnetic force and experiments in electromagnetic forming with local loading," *Int. J. Appl. Electromagn. Mech.*, vol. 57, no. 1, pp. 29–37, Apr. 2018.
[11] Y. Kiliclar, O. K. Demir, I. N. Vladimirov, L. Kwiatkowski, A. Brosius, S. Reese, and A. E. Tekkaya, "Combined simulation of quasi-static deep drawing and electromagnetic forming by means of a coupled damage-viscoplasticity model at finite strains," in *Proc. 5th Int. Conf. High Speed Forming*, Dortmund, Germany, 2012, pp. 325–333.
[12] X. Cui, J. Mo, J. Li, J. Zhao, Y. Zhu, L. Huang, Z. Li, and K. Zhong, "Electromagnetic incremental forming (EMIF): A novel aluminum alloy sheet and tube forming technology," *J. Mater. Process. Technol.*, vol. 214, no. 2, pp. 409–427, Feb. 2014.
[13] L. Li, X. T. Han, and Q. L. Cao, "Development of space-time-controlled multi-stage pulsed magnetic field forming and manufacturing technology at the WHMFC," in *Proc. 6th Int. Conf. High Speed Forming*, Daejeon, South Korea, 2014, pp. 353–362.
[14] Z. Lai, Q. Cao, B. Zhang, X. Han, Z. Zhou, Q. Xiong, X. Zhang, Q. Chen, and L. Li, "Radial Lorentz force augmented deep drawing for large drawing ratio using a novel dual-coil electromagnetic forming system," *J. Mater. Process. Technol.*, vol. 222, pp. 13–20, Aug. 2015.
[15] L. Qiu, Y. Yu, Q. Xiong, C. Deng, Q. Cao, X. Han, and L. Li, "Analysis of electromagnetic force and deformation behavior in electromagnetic tube expansion with concave coil based on finite element method," *IEEE Trans. Appl. Supercond.*, vol. 28, no. 3, pp. 1–5, Apr. 2018.
[16] Z. Li, C.-F. Li, H.-P. Yu, and Z.-H. Zhao, "Effect of tube size on electromagnetic tube bulging," *Trans. Nonferrous Metals Soc. China*, vol. 17, no. 4, pp. 705–710, Aug. 2007.
[17] Z. Li, S. Li, L. Li, and M. Wang, "Effect of coil length and relative position on electromagnetic tube bulging," *Int. J. Adv. Manuf. Technol.*, vol. 97, pp. 379–387, Mar. 2018.
[18] X. Cui, J. Mo, J. Li, and X. Xiao, "Tube bulging process using multidirectional magnetic pressure," *Int. J. Adv. Manuf. Technol.*, vol. 90, nos. 5–8, pp. 2075–2082, May 2017.
[19] L. Qiu, Y. Yu, Z. Wang, Y. Yang, Y. Yang, and P. Su, "Analysis of electromagnetic force and deformation behavior in electromagnetic forming with different coil systems," *Int. J. Appl. Electromagn. Mech.*, vol. 57, no. 3, pp. 337–345, Jun. 2018.
[20] L. Qiu, Y. Li, Y. Yu, Y. Xiao, P. Su, Q. Xiong, J. Jiang, and L. Li, "Numerical and experimental investigation in electromagnetic tube expansion with axial compression," *Int. J. Adv. Manuf. Technol.*, vol. 104, nos. 5–8, pp. 3045–3051, 2019.
[21] J. Wheeler, J. Dean, and T. Clyne, "Nano-impact indentation for high strain rate testing: The influence of rebound impacts," *Extreme Mech. Lett.*, vol. 26, pp. 35–39, Jan. 2019.
[22] J. Thomas, M. Seth, G. Daehn, J. Bradley, and N. Triantafyllidis, "Forming limits for electromagnetically expanded aluminum alloy tubes: Theory and experiment," *Acta Mater.*, vol. 55, no. 8, pp. 2863–2873, May 2007.

LI QIU (Member, IEEE) received the B.S., M.S., and Ph.D. degrees in electrical engineering from the Huazhong University of Science and Technology, Wuhan, China, in 2012.

He is currently an Associate Professor with the College of Electrical Engineering and New Energy, China Three Gorges University, Yichang. He is the author of more than 15 articles, and more than 10 inventions. His research interests include the technology of pulsed high magnetic field, high voltage technology, and electromagnetic forming. He is a Periodical Reviewer of the IEEE TRANSACTIONS ON APPLIED SUPERCONDUCTIVITY and *International Journal of Applied Electromagnetics and Mechanics*.

WANG ZHANG is currently pursuing the master's degree majoring in control science and engineering with the College of Electrical Engineering and New Energy, China Three Gorges University, Yichang.

A. ABU-SIADA (Senior Member, IEEE) received the B.Sc. and M.Sc. degrees from Ain Shams University, Egypt, in 1998, and the Ph.D. degree from Curtin University, Australia, in 2004, all in electrical engineering.

He is currently an Associate Professor and the Discipline Lead of the electrical and computer engineering at Curtin University. His research interests include power electronics, power system stability, condition monitoring, and power quality. He is the Editor-in-Chief of the *International Journal of Electrical and Electronic Engineering* and a regular reviewer for various IEEE TRANSACTIONS. He is the Vice-Chair of the IEEE Computation Intelligence Society and WA Chapter.

QI XIONG (Member, IEEE) received the B.S., M.S., and Ph.D. degrees in electrical engineering from the Huazhong University of Science and Technology, Wuhan, China, in 2016. He is currently a Lecturer with the College of Electrical Engineering and New Energy, China Three Gorges University, Yichang. His research interests include the technology of pulsed high magnetic field, high voltage technology, and electromagnetic forming.

CHENGLIN WANG is currently pursuing the degree in electrical engineering with the College of Electrical Engineering and New Energy, China Three Gorges University, Yichang.

YAO XIAO is currently pursuing the degree with State Grid Jilin Electric Power Company, Ltd., and Changchun Power Supply Company, Changchun, China.

BIN WANG is currently pursuing the degree in electrical engineering with the College of Electrical Engineering and New Energy, China Three Gorges University, Yichang.

YANTAO LI is currently pursuing the degree with State Grid Yiling Power Supply Company, Yichang, China.

JINBO JIANG received the B.S. degree from the College of Mechatronics and Control Engineering, Hubei Normal University, Huangshi, China, in 2010.

He is currently a Lecturer with the College of Electrical Engineering and New Energy, China Three Gorges University, Yichang. His research interests include the technology of pulsed high magnetic field, high voltage technology, and pulsed power technology.

QUANLIANG CAO received the B.S. and Ph.D. degrees from the School of Electrical and Electronic Engineering, Huazhong University of Science and Technology (HUST), in 2008 and 2013, respectively. He is currently an Associate Professor with HUST. His research interests focus on the object manipulation using magnetic fields, including electromagnetic forming, magnetic separation, and magnetic microrobots.